Transactions, SMiRT-25
Charlotte, NC, USA, August 4-9, 2019
Division V

NUMERICAL STUDY ON SEISMIC PERFORMANCE OF SHEAR WALL AFTER HIGH TEMPERATURE EXPOSURE

Hiroshi Tomofuji[1], Yuki Sasaki[1], Takaaki Tsukada[1], Mario Fontana[2]

[1] Nuclear Projects Division, Shimizu Corporation, Kyobashi Chuo-ku, Tokyo, JAPAN
(h_tomofuji@shimz.co.jp)
[2] Professor, ETH Zurich, Zurich, SWITZERLAND

ABSTRACT

As concrete structures may have a risk to be exposed to various elevated temperature which is different from ISO fire curve, the different temperature hysteresis may cause different deterioration of concrete. As residual structural performance of shear walls may be different from those confirmed by concrete cylinder tests, loading test on the shear wall which experienced high temperature exposure was implemented [Horigome et al. (2016) and Sasaki et al. (2016)] and the structural behaviour subjected to subsequent cyclic horizontal loading was demonstrated by 3D FEM nonlinear analysis [Mori et al. (2016)]. [Horigome et al. (2016) and Sasaki et al. (2016)] showed that the maximum shear capacity of degraded wall could be assumed by truss-arch theory. [Mori et al. (2016)] showed that the accuracy of cyclic loading analysis on degraded concrete could be improved by taking the effect of thermal cracking which was evaluated by simple thermal stress analysis into account as an initial condition. However, the mechanical properties (strength and stiffness) of degraded concrete used in these analytical studies were obtained directly from the concrete cylinder which experienced actual high temperature exposure. The temperature distribution inside the shear wall to be used for the simple thermal stress analysis was also based on the test data. It would be difficult to measure the temperature distribution inside the actual structure or extract the concrete cylinder from the structure to get the degraded concrete mechanical properties. In this study, detailed heat transfer analysis and stress analysis are performed and the degradation of concrete is developed based on the numerous researches or design code. Furthermore, the behaviour of shear wall subjected to cyclic horizontal loading after high temperature exposure is demonstrated by utilizing the degradation of concrete obtained from these analyses.

INTRODUCTION

ISO fire curve [ISO834(1975)] is one of common high temperature hysteresis to confirm concrete properties at elevated temperature. As concrete structures may have a risk to be exposed to various elevated temperature which is different from ISO fire curve, the different temperature hysteresis may cause different deterioration of concrete. To confirm the effect of elevated temperature exposure on the concrete properties, experimental study was performed by concrete cylinders [Eike et al. (2012)]. The results showed that concrete properties were further degraded by cooling process.

It is common to install thick concrete shear walls to meet shielding and seismic performance requirements in the nuclear facilities. If concrete shear walls are exposed to elevated temperature, residual structural performance of shear walls may be different from those confirmed by concrete cylinder tests. An experimental study of concrete shear walls pre-damaged by high temperature exposure was implemented in 2016 [Horigome et al. (2016) and Sasaki et al. (2016)].

Mori et al. (2016) demonstrated the behaviour of concrete wall subjected to cyclic loading by numerical simulation by using 3D FEM program in consideration with material nonlinearity and material degradation caused by high temperature exposure. The study showed that the analysis results were improved by introducing the effect of crack which was evaluated by simple thermal stress analysis. In this

paper, a numerical study of concrete shear walls is performed in combination with detail heat transfer, thermal stress and pushover analyses in succession. Differences between test results and analysis results are compared to adopt the different parameters from the conventional study [Tomofuji and Sasaki(2017)].

EXPERIMENTAL STUDY

Overview

Pre-damage heating and post-damage horizontal loading tests were implemented on concrete shear wall [Horigome et al. (2016) and Sasaki et al. (2016)]. The dimension of specimen and manufacture process is illustrated in Figure 1. The specimen has "I-shaped" shear wall in a horizontal projection and consists of flanges and a web. The heating test is carried out only for the web then horizontal loading test is performed for the "I-shaped" shear wall. The idea to attach the flanges is to enhance shear capacity and avoid brittle failure under horizontal loading. As described in Figure 1, the web is attached to flanges and massive upper and lower concrete volumes, i.e. upper stub and lower stub, which are casted after the heating test. The dimensions of rectangular solid web are 900mm high, 800mm wide and 300mm thick, which are scaled down to approximately 1:6 due to the limitation of lifting device capacity in the laboratory. The web is embedded into the flanges by 50mm depth and also embedded into the stubs by 100mm depth to provide sufficient rigidity.

Table 1 shows experimental parameters. As described in Figure 1, two types of high temperature exposure are considered to confirm seismic performance of various shear walls. One is exposed to high temperature exposure at one wide surface and the other is exposed to high temperature exposure at both two wide surfaces. According to the conventional study, the deterioration of concrete becomes obvious when specimen is exposed to heat more than 300˚C because micro crack inside of concrete is permanently formed [Guide book for fire-resistive performance of structural materials (2017)]. When a specimen is exposed to heat between 400 to 600˚C, material properties are further deteriorated because crystal hydroxide ($Ca(OH)_2$) decomposed in to Calcium oxide(CaO) and water [Hertz (2005)]. Therefore, maximum target temperature is set as 600˚C for both specimens to evaluate moderate deterioration by high temperature exposure.

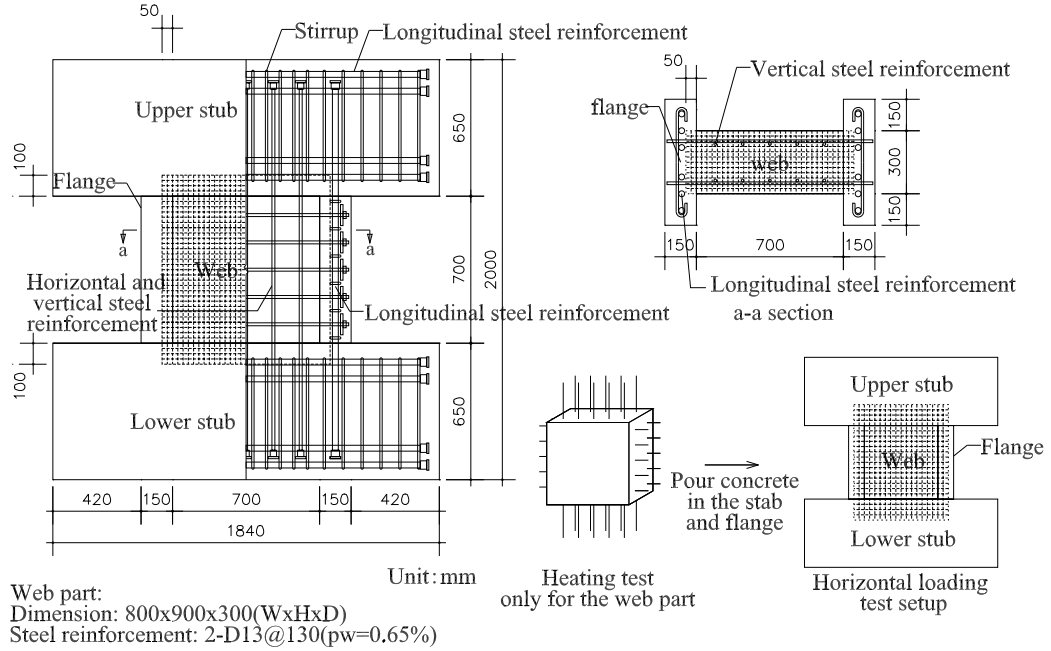

Figure 1. The dimension of specimen and manufacture process.

Table 1: Experimental parameters.

Specimen	Heating side	Maximum target temperature
600o	One wide surface	600˚C
600b	Two wide surface	600˚C

Heating Test

The temperature hysteresis curve is shown in Figure 2. Maximum temperature is set as 600˚C and heating test is only performed for the web only. After the heating test, the webs are left at room temperature approximately for 2 months. The web is heated up by a ceramic heater at a distance of 30mm and covered with insulation all narrow surfaces around to prevent heat emission. The concept of temperature hysteresis curves consist of three steps such as one heating and two cooling phases.

1) Heating phase
   The heating speed controlled by the furnace is 100˚C to 200˚C per hour and each specimen is kept at the maximum temperature within designated hours to make sure until the temperature variation between the inside and the surface becomes negligible.
2) Cooling phase 1
   As a former cooling phase, the power supply of furnace is just switched off to wait until the surface of the specimen becomes lower than 300˚C. The reason to have former cooling phase is to decrease thermal stress without abrupt cooling. As the abrupt cooling causes high temperature difference between the inner and the surface, that might possibly cause further deterioration of concrete properties.
3) Cooling phase 2
   As a latter cooling phase, the specimen is left apart from the heater to wait until the temperature of the surface decreased to room temperature. The reason to have latter cooling phase is to optimize time efficiency because the temperature difference between the inner and the surface below 300˚C is considered as insignificant.

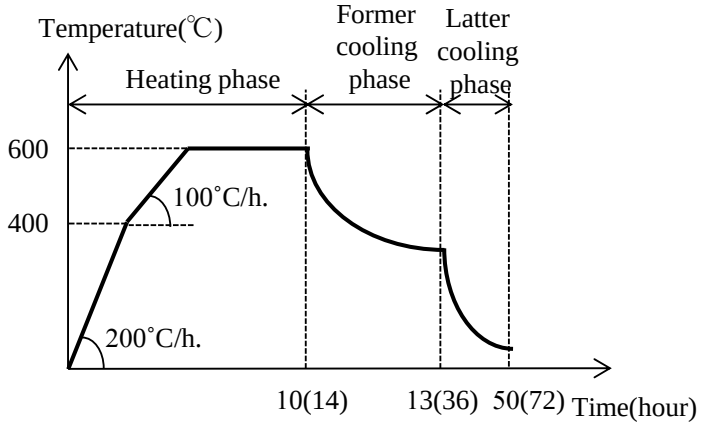

( ) indicates temperature hysteresis curve for specimen 600b.
Figure 2. Temperature hysteresis curve.

Horizontal Loading Test

The horizontal load is applied to the specimens by hydraulic jacks after exposing elevated temperature to the webs. Horizontal loading setup [Horigome et al. (2016)] and loading protocol is illustrated in Figure 3. Two vertical hydraulic jacks are controlled by displacement without axial load and two vertical jacks are kept at same length to make the inflection height set at the centre of the web. Two horizontal hydraulic jacks are controlled by displacement to have cyclic loading twice up to 0.004 radian of a deflection angle.

The deflection angle is obtained the relative displacement between the upper and lower stubs divided by the distance between upper and lower stubs, i.e. 700mm. Furthermore, the horizontal shear force is measured by load cells attached between horizontal hydraulic jacks and the loading frame.

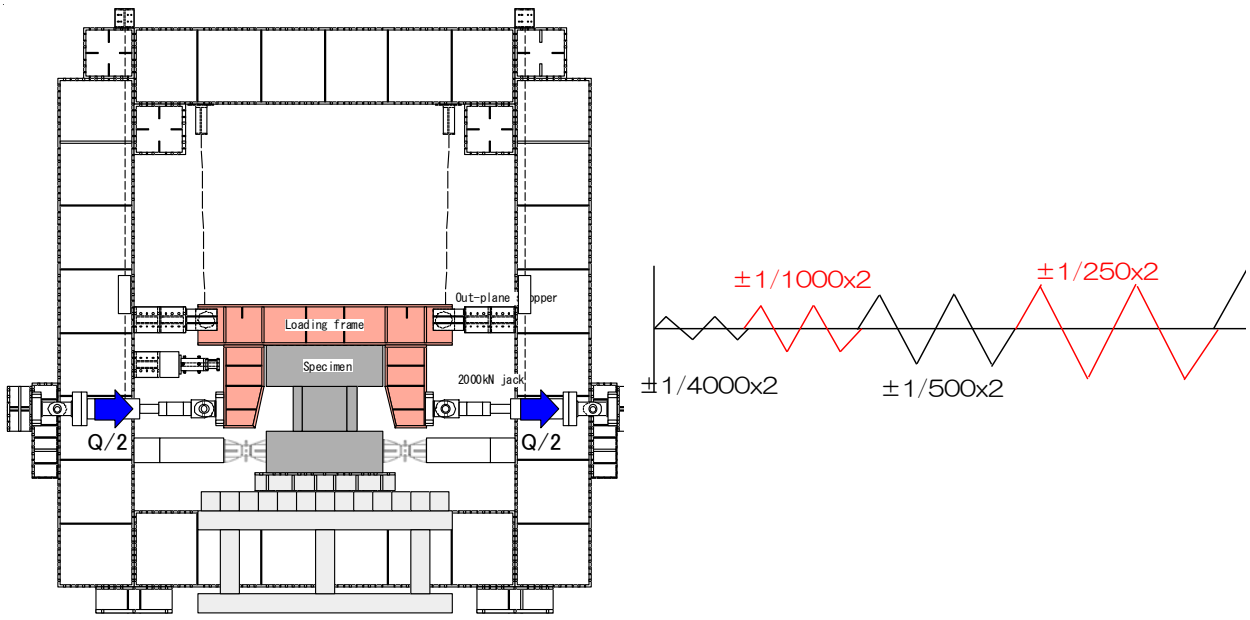

(a) Horizontal loading test setup (b) Loading protocol

Figure 3. Horizontal loading test setup and loading protocol.

NUMERICAL STUDY

Prior to this study, Mori et al. (2016) performed 3D FEM nonlinear analysis by using multi-layered shell model to demonstrate the test results introduced above. In the previous study, the degraded concrete material properties were based on the concrete cylinder test results which experienced actual high temperature exposure in the test. Separate simple thermal stress analysis without steel reinforcement was performed by applying the measured temperature distribution in the test to evaluate the cracking depth which was taken into account in the cyclic horizontal loading analysis.

Figure 4 shows 3D FE models and test setups in this study. The numerical simulation is performed by ABAQUS/Standard [ABAQUS (2015)]. To capture the experimental study accurately including heating and horizontal loading tests, different 3D FEM models are prepared. As described in Figure 4(a), the web is modelled as solid elements and the steel reinforcement is modelled as bar elements. The steel reinforcement is embedded into the web and full rigidity between steel reinforcement and neighbouring concrete elements is assumed.

For the heat transfer analysis, a heater is modelled as shell elements. Heat radiation and heat convection is considered between the heater and the web. In terms of thermal conductivity and specific heat of concrete, upper limit value of the code [EUROCODE 2 (2004)] and 3% moisture content is considered respectively. Coefficients for heat convection on the heating side or the opposite non-heating side were defined as 25W/m^2, 12 W/m^2 respectively.

After the heat transfer analysis, thermal stress and pushover analyses are performed by importing the results obtained by previous analyses. For the thermal stress analysis and pushover analysis, material nonlinearity of concrete is considered. Concrete damage plasticity model is adopted to take into account of deterioration of concrete as a scalar. Table 2 provides material test results and design values. Different design strength is assumed for the web and flanges. Maximum compressive strength for the web is provided as 42.2MPa based on the material test results and the tensile strength is assumed in accordance

with the reference [Horigome et al. (2016)]. Details of constitutive law of the concrete portion exposed to elevated temperature is provided in the reference[Tomofuji and Sasaki(2017)]. EUROCODE 2 (2004) provides the uniaxial compressive stress-strain relationship both pre-peak and post-peak regimes. Concrete properties are deteriorated if a specimen is exposed to elevated temperature. Reduction factor of compressive strength at elevated temperature is defined in accordance with Hertz[Hertz(2005)] and that of tensile strength at elevated temperature is defined in accordance with EUROCODE 2 (2004). The bonding parameter *c* in the tension softening behaviour is set as 0.4 in accordance with Izumo model [Izumo et al. (1987)] (concrete with steel reinforcement). The stiffness degradation coefficient in compression and in tension are also adopted as 0.8 and 0.7 respectively [Birtel(2005), Tomofuji and Sasaki(2017)]. The change of concrete properties is permanent if the specimen which is exposed to elevated temperature was cooled down to ambient temperature [Hertz (2005)]. To take the maximum experienced temperature dependency into account as a constitutive law, ABQAQUS user subroutine is used. In addition to the conventional study [Tomofuji and Sasaki(2017)], adopted thermal elongation of concrete is described latter in "Thermal Stress Analysis" section.

For steel reinforcement, material test results and design values are also provided. The true stress and true strain relationship is assumed based on the material test results. Furthermore, thermal elongation of steel reinforcement is defined in accordance with the code [EUROCODE 3 (2005)].

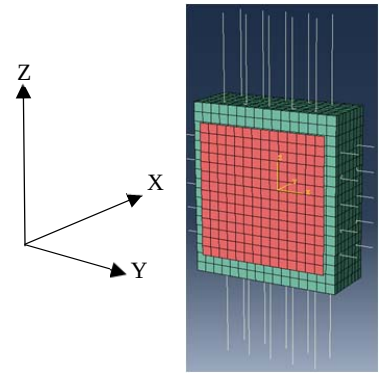

(a) Heat transfer and thermal stress analysis model(Red colored shell: *Heater*, Green colored solid: *Web part*)

(b) Heating test setup

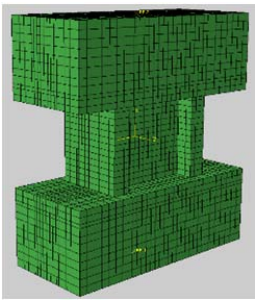

(c) Pushover analysis model

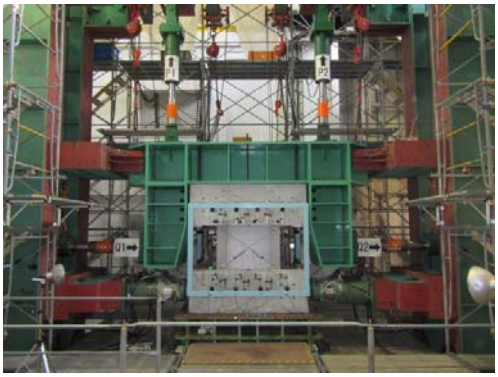

(d) Loading test setup

Figure 4. 3D FEM models and test setups.

Table 2. Material test results and design values.

Material	Concrete		Steel reinforcement		
	Compressive strength(N/mm^2)		Yield strength(N/mm^2)		
	Web	Flanges	Longitudinal bar for web	Longitudinal bar for flanges	Stirrups
Design value	33.0	48.0	345	390	294
Test results	42.2	56.1	415	466	384

HEAT TRANSFER ANALYSIS

Figure 5 shows the comparisons of temperature hysteresis curve between test and analysis. Though total 45(9x5) thermocouples were embedded in each specimen, the results at red highlighted 5 points described in Figure 5(b) aligned at the centre of web through its thickness were compared between test and analysis. For the specimen 600b, only 3 results (A, B and C) compared because both wide surfaces exposed to elevated temperature symmetrically. The target temperature time history in the heater (black line) also shown in Figure 5. Numerical analysis result showed a good agreement with experimental result for adopted 5 thermocouple measurement in both heating and cooling phases.

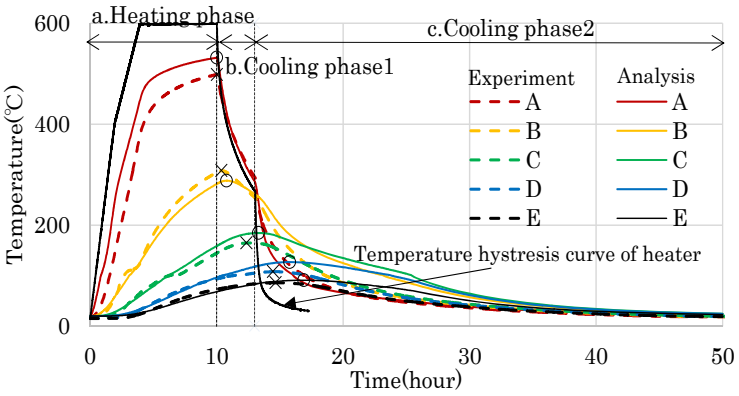

(a) Specimen 600o

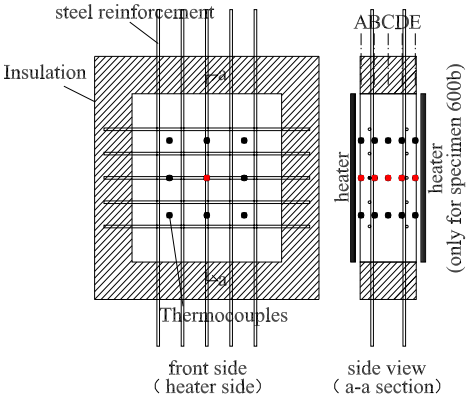

(b)references

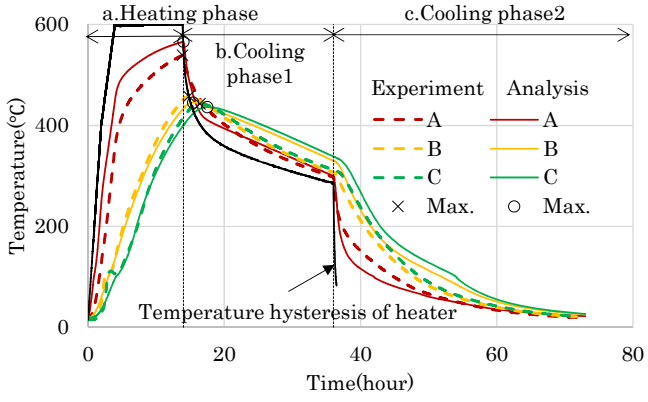

(c) Specimen 600b

Figure 5. Temperature hysteresis curve between test and analysis.

THERMAL STRESS ANALYSIS

Figure 6 shows the comparisons of strain of steel reinforcement between test and analysis. As described in Figure 6(b), two strain gauges attached at the steel reinforcement in each specimen. Two strain gauges located closely to the heated wide surface. Adopted thermal elongation $\varepsilon_c(\theta)$ of concrete shown in Figure 6(d) slightly larger than that in EUROCODE 2 (2004).

$$\varepsilon_c(\theta) = -1.8 \times 10^{-4} + 9.0 \times 10^{-6}\theta + 2.8 \times 10^{-11}\theta^3 \quad (1)$$

Where $\varepsilon_c(\theta)$ is the thermal elongation, θ is the temperature ($^{\circ}$C; $20^{\circ}\text{C} \leq \theta \leq 700^{\circ}\text{C}$).

If no residual thermal elongation was assumed, thermal elongation after removal of high temperature exposure was zero (0). As the residual thermal elongation was confirmed after high temperature exposure by the experimental study [Tomofuji et al. (2019)], the coefficient of increment of thermal elongation in the cooling phase was set as 1.5-2.0 though that in the heating phase 1.0 in the ABAQUS user subroutine described as per Figure 6(d).

Thermal elongation of concrete had similar tendency with that of steel reinforcement up to 400°C as described in Figure 6(d). When specimens were exposed to elevated temperature, the strains of steel reinforcement were large in the tensile regimes for both specimens. This is because heat convection transferred from the heated concrete to the neighbouring steel reinforcement and the strain of steel reinforcement needs to satisfy compatibility between the heated concrete and neighbouring the steel reinforcement. For the specimen 600o, the strain was decreased in the cooling phase 1 whereas the different tendency was observed for specimen 600b as the strain was almost constant in the cooling phase1. Though the strain reduction of steel reinforcement for specimen 600o in the cooling phase1 was well captured by the corresponding thermal stress analysis, that for specimen 600b was not captured. The

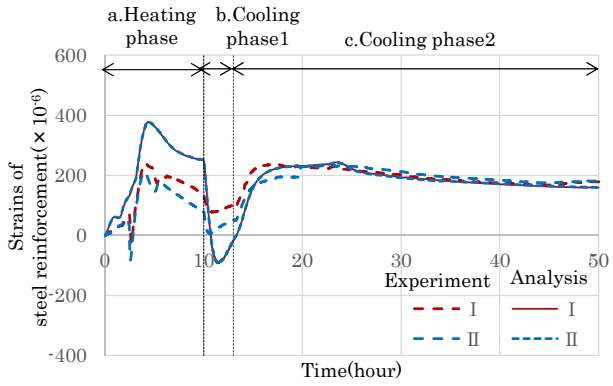

(a) Specimen 600o

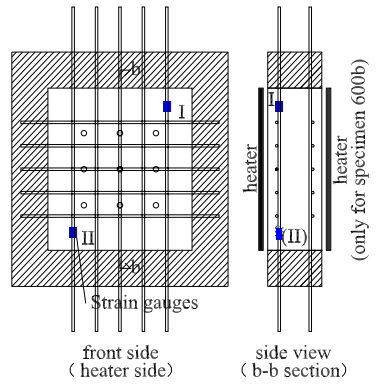

(b)references

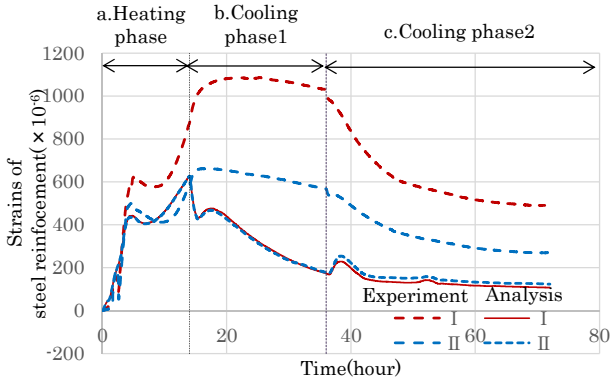

(c) Specimen 600b

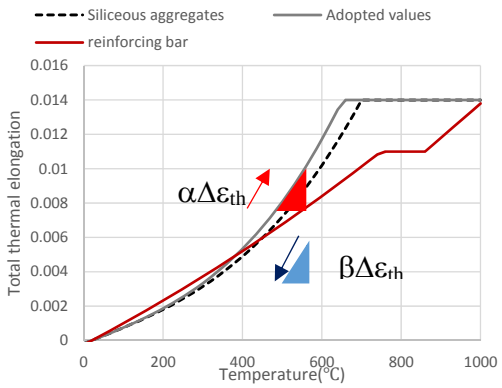

(d)Adopted thermal elongation of concrete

Figure 6. Strain of steel reinforcement between test and analysis.

reason was considered that the bond capacity apparently was decreased due to longer duration of high temperature exposure compared to the specimen 600o [Kumagai et al.(1992)].

Table 2 shows the comparisons of crack pattern at the wide surfaces between test and analysis. With regard to the specimen 600o, cracks were only observed on the heated wide surface but no crack was observed on the opposite unheated wide surface. As cracks were observed during the cooling phase in the test, this tendency was captured by the thermal stress analysis. Though the plastic maximum principal strain did not directly indicate the crack width and length, it can be used as a factor to comprehend the tendency of crack pattern. Obtained numerical results had good agreement with test results as larger plastic maximum principal strain was observed in the cooling phase, which caused the crack propagation.

Table 2: Crack pattern at the wide surfaces between test and analysis.

(a1)The heated surface

(a2)The unheated surface

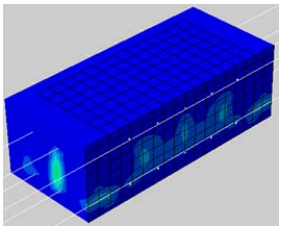

(a3)Analytical distribution after heating phase

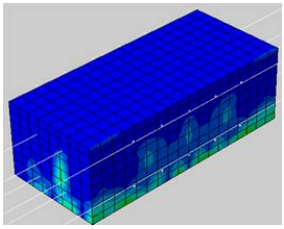

(a4)Analytical distribution after cooling phase2

(a)Specimen 600o

(b1)The heated surface

(b2)Another heated surface

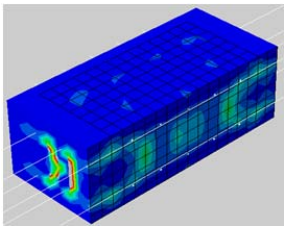

(b3)Analytical distribution after heating phase

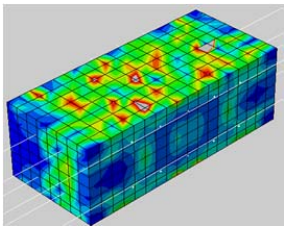

(b4)Analytical distribution after cooling phase2

(b)Specimen 600b

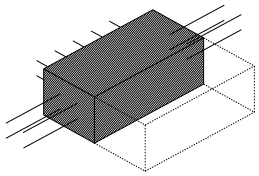

Grey-colored half-sized model of the web

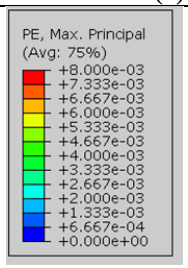

Contour reference

1) tensile strain:+, compressive strain:-
2) The results are provided only for grey-colored half-sized model of the web described left.

PUSHOVER ANALYSIS

The pushover analysis was performed for both specimens, in which the results of thermal stress analysis was taken over to the pushover analysis as an initial condition. In the pushover analysis, upper stab was

controlled by displacement and given displacement was increased monotonically up to 0.025 radian deflection angle. Figure 7 shows the comparisons of results between pushover analysis and horizontal loading test. Figure 7 also showed the analysis results of previous study implemented by Mori et al. (2016). The numerical analysis results had similar result to the experimental results. Maximum plastic principal strain distribution at final failure condition showed good agreement with the crack pattern observed in the loading test.

Compared to the numerical analysis results of this study with the previous study by Mori et al. assessed by separate simple thermal stress analysis in the previous study, the maximum shear strength was improved by evaluating the effect of thermal stress explicitly with the detail FE model and taking the stress and strain condition over to the subsequent pushover analysis.

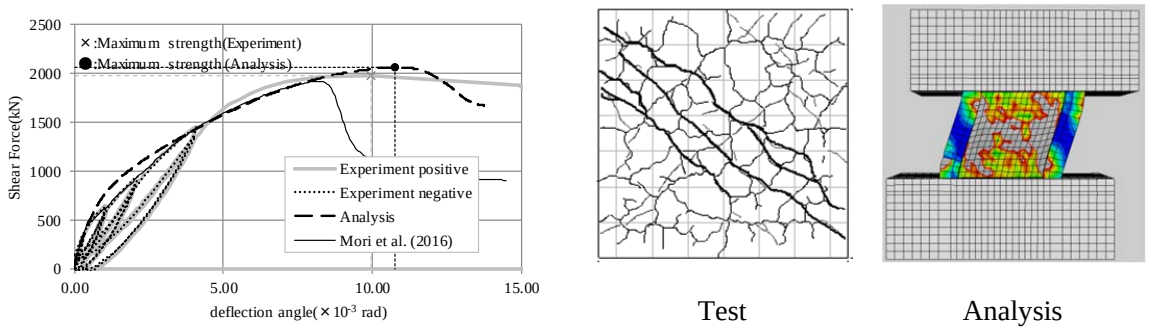

(a1)Q-δ curve

(a2) Maximum plastic principal strain and test crack distributions

(a) Specimen 600o

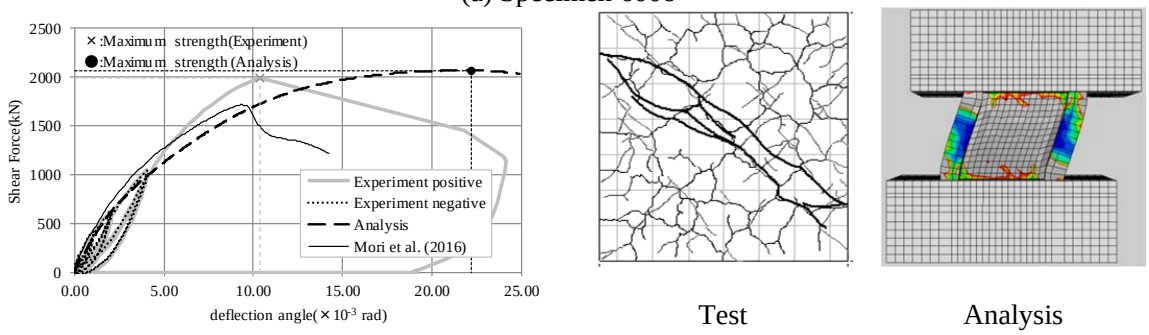

(b1)Q-δ curve

(b2) Maximum plastic principal strain and test crack distributions

(b) Specimen 600b

Figure 7. The relationship between shear force and deformation angle between test and analysis.

CONCLUSION

This paper presented numerical study on seismic performance of shear wall after high temperature exposure. Series of numerical study such as heat transfer, thermal stress and pushover analyses performed and the results were compared with corresponding experimental results. The major findings were summarised as follows;

1. Heat transfer and thermal stress analyses were performed. Temperature hysteresis curves obtained by analyses showed good correlations with those obtained by tests. As major cracks were observed in the cooling phase of tests, this tendency also observed in the analysis results.
2. To combine material nonlinearity with degradation of mechanical properties of concrete exposed to elevated temperature, constitutive law of concrete was expanded by using ABAQUS user subroutine. Established simulation method confirmed with experimental results proved to be effective because numerical results captured the global behaviour of test results.

3. By introducing the established simulation method, the structural behaviour of reinforced concrete shear wall with degraded concrete by high temperature exposure can be demonstrated without concrete cylinder testing with the specimen extracted from the actual structure and thermal distribution data inside the wall.
4. As shown in Figure 6 (c), the strain of steel reinforcement under long term high temperature exposure showed variance from the numerical analysis result. The loss of bond between steel reinforcement and the neighbouring concrete should be properly treated in the analysis in such case.

ACKNOWLEDGEMENT
The writer is grateful to Mr. Kazuaki Igaki of Lattice for the implementation of ABAQUS user subroutine in this study.

REFERENCES
ABAQUS version 6.13 (2015). *ABAQUS user manual*, SIMULIA Inc. U.S.A.
Birtel, V. and Mark.P. (2006). Parameterised finite element modelling of RC beam shear failure, *ABAQUS User's Conference*.
EUROCODE 2 (2004). *Eurocode2: Design of Concrete Structures-Part 1-2: General Rules, Structural Fire Design*. EN1992-1-2, European Committee for Standardization.
EUROCODE 3 (2005). *Eurocode3: Design of Steel Structures-Part1-2; General Rules- Structural Fire Design*. EN1993-1-2, European Committee for Standardization.
Hertz, K.D. (2005). "Concrete strength for fire safety design", *Magazine of Concrete Research*, Institute of Civil Engineering, Vol. 57, No. 8, pp. 445-453.
Horigome, K., Sasaki, Y., Nishimura, T., Sakazume, Y., Hirama, T and Kurosawa, I. (2016). "Study on seismic performance of RC shear walls exposed to high temperature, Part 1 Outline of experiment and results of material test", *Annual Convention of Architectural Institute of Japan* (in Japanese).
ISO-834 (1975). "Fire resistance test-elements of building construction". *International Standard ISO834*, Geneva, Switzerland.
Izumo, J. Shima, H. and Okamura, H. (1987). "Analytical model of RC shell element under in-plane stress", *Journal of Concrete Institute*, Vol.25,No.9(in Japanese).
Klingsch, E., Frangi, A. and Fontana, M. (2012). "Ordinary and High-performance concrete; Hot strength and residual strength after cooling from high temperatures", *Befestigungstechnik Bewehrungs-technik und II Rolf Eligehausen zum 70. Geburtstag*.
Kumagai, H., Saito, H. and Morita, T. (1992). "Mechanical properties of high performance concrete after high temperature exposure", *Annual Convention of Japan Concrete Institute*. Vol.14, No.2.
Mori, Y., Sasaki, Y., Sakazume, Y., Kurosawa, I., Tomofuji, H. and Kumagai, H. (2016). "Study on seismic performance of RC shear walls exposed to high temperature, Part3 Simulation analysis", *Annual Convention of Architectural Institute of Japan*. (in Japanese).
Sasaki, Y., Nishimura, T., Horigome, K., Hirama, T., Kurosawa, I. (2016). "Study on seismic performance of RC shear walls exposed to high temperature, Part2 Results of experiment –heating test and shear loading test", *Annual Convention of Architectural Institute of Japan*. (in Japanese).
Tomofuji, H. and Sasaki, Y. (2017). "Analytical study on residual seismic performance of RC Shear wall after pre-damaged by high temperature exposure", P*roceedings of The Eleventh High Performance Concrete (11th HPC) & The Second Concrete Innovation Conference (2nd CIC)*. Tromsø. Norway.
Tomofuji, H., Morita, T., Watanabe, K., Yamada, S. and Hayashi, A. (2019). "Experimental Study on Residual Mechanical Properties of Concrete after high temperature exposure under axially loaded condition", *Structural Mechanics In-Reactor Technology 25*. Charlotte. USA.